A general model for temperature-dependence in biology

José Ignacio Arroyo (1)*, Beatriz Díez(2,3,4), Chris Kempes(5), Geoffrey B. West(5), and Pablo A. Marquet(1,6,7,8)

(1) Departamento de Ecología, Facultad de Ciencias Biológicas, Pontificia Universidad Católica de Chile, CP 8331150, Santiago, Chile.

(2) Departamento de Genética Molecular y Microbiología, Facultad de Ciencias Biológicas, Pontificia Universidad Católica de Chile, CP 8331150, Santiago, Chile.

(3) FONDAP Center for Climate and Resilience Research, University of Chile, Santiago, Chile

(4) FONDAP Center for Genome Regulation, Faculty of Science, University of Chile, Santiago, Chile

(5) The Santa Fe Institute, 1399 Hyde Park Road, Santa Fe NM 87501, USA.

(6) Instituto de Ecología y Biodiversidad (IEB), Las Palmeras 3425, Santiago, Chile.

(7) Centro de Cambio Global UC, Facultad de Ciencias Biológicas, Pontificia Universidad Católica de Chile, CP 8331150, Santiago, Chile.

(8) Instituto de Sistemas Complejos de Valparaíso (ISCV), Subida Artillería 470, Valparaíso, Chile.

Corresponding authors:José Ignacio Arroyo, E-mail: jiarroyo@uc.cl and Pablo Marquet, E-mail: pmarquet@bio.puc.cl

* Current Address: The Santa Fe Institute, 1399 Hyde Park Road, Santa Fe NM 87501, USA; Centro de Modelamiento Matemático, Universidad de Chile - IRL 2807 CNRS Beauchef 851, Santiago, Chile.

Abstract

Temperature affects all biological rates and has far reaching consequences from bioengineering [1] to predicting ecological shifts under a changing climate [2-3], and more recently, to pandemic spread [4]. Temperature response in biological systems is characteristically asymmetric and nonlinear, with an exponential phase of increase followed by a concave upward or downward phase [5]. Current models for quantitatively describing the temperature response include simple but empirical equations (such as Arrhenius') or models derived from first principles which are often overly complicated (i.e. with many parameters). Moreover, their theoretical framework does not include how parameters vary, nor their applicability across multiple scales and taxa, or whether they exhibit universality [1-7]. Here, we derive a new mechanistic, yet simple, model for the temperature dependence of biological rates based on the Eyring-Evans-Polanyi theory governing chemical reaction rates, which is applicable across all scales from the micro to the macro. Assuming only that the conformational entropy of molecules changes with temperature, we derive a model for the temperature dependence which takes the form of an exponential function modified by a power-law. Data for a wide variety of biological rates from molecular to ecological scales and across multiple taxonomic groups agree well with our predictions. Furthermore, our framework predicts values for the thermodynamic parameters, and leads to a single parameterless universal scaling curve on which data across all scales and taxa collapse.

Main Text

Temperature dependence models and the Eyring-Evans-Polanyi (EEP) theory. Temperature affects reaction rates of enzymes, which regulate processes that manifest at all levels of biological organization from molecules to ecosystems [1-7]. The classic Arrhenius equation [8-9] for the temperature dependence of chemical reaction rates (k), has become the standard mathematical description of temperature responses used by biologists and ecologists, as epitomized, for example, by the Metabolic Theory of Ecology (MTE), [7] and is given by

$$k = ae^{-E/k_BT} \tag{1}$$

where k_B is Boltzmann's constant, T is absolute temperature, E is an effective activation energy for the process of interest, and a is an overall normalization constant characteristic of the process. Consequently, a plot of $\log k$ vs. $1/T$ should yield a straight line, often referred to as an Arrhenius plot. This equation was originally an empirical formulation, but was later motivated heuristically from chemical reaction theory [10] (see Supplementary Text S1). Although it has been instrumental in explaining the approximately universal temperature dependence across many diverse biological rates [5, 7], it cannot account for deviations that occur beyond certain temperature ranges in, for example, the metabolic rates of endotherms, thermophiles and hyperthermophiles [3, 5, 11]. Furthermore, experiments and observations have established that the form of the temperature response has an asymmetric concave upward or downward pattern relative to a canonical straight-line Arrhenius plot [1-7].

Despite the widespread use of the Arrhenius equation in biology, the EEP Transition State Theory (TST) [12-13] is the widely accepted model of enzyme chemical kinetics, as it is grounded in the underlying principles of equilibrium thermodynamics, kinetic theory and statistical physics [14]. The framework of the TST conceives of a chemical reaction as a flux of molecules with a distribution of energies and a partition function given by the Planck distribution, flowing through a potential energy surface (PES) which effectively simulates their interaction. The configuration of molecules flowing through this surface proceeds from i) a separate metabolite and enzyme to ii) an unstable metabolite-enzyme complex, which, iii) after crossing a critical energy threshold barrier, or transition state, then forms the final product (the transformed metabolite). EEP thereby derived the following equation for the reaction rate (see Supplementary Text S2):

$$k = \frac{k_B}{h}Te^{-\Delta G/RT} \tag{2}$$

where h is Planck's constant, ΔG is the change in Gibbs energy or free enthalpy, $R = Nk_B$ is the universal gas constant and N Avogadro's number. An overall coefficient of transmission also is originally part of (2) but is usually assumed to be 1. The change in Gibbs free energy is the energy (heat) transferred from the environment to do chemical work. It can be expressed in terms of enthalpy (ΔH) and the temperature-dependent change in entropy, or dissipated energy (ΔS) [15], as $\Delta G = \Delta H - T\Delta S$. Eq. (2) can then be written as:

$$k = \frac{k_B}{h}Te^{\Delta S/R}e^{-\Delta H/RT} \tag{3}$$

Analogous to the Arrhenius expression, Eqs. (2) and (3) describe an exponential response in the rate k to temperature provided there is no temperature dependence of the thermodynamic parameters. Models have been developed for including this additional temperature dependence, but they typically invoke several additional assumptions and new parameters [16-17] (Supplementary Text S1). Furthermore, unlike the widespread use of the Arrhenius equation in the MTE, most models for temperature response have been conceived for a single level of biological organization (commonly at the enzymatic molecular level) [6, 17] or for specific taxonomic groups; e.g. only for mesophilic ectotherms [18], for endotherms [19], or thermophiles [20]. Here, we present a relatively simple general mechanistic model for these temperature effects in biology [3, 6, 11] which is applicable across multiple levels of biological organization and taxa (see discussion in Supplementary Text S1) and which gives a natural explanation for the concave/convex deviations from the classic Arrhenius straight line. Furthermore, we show how the parameters of the model can be quantitatively derived and how data for various variables can be collapsed onto a single "universal" curve, reflecting the generality of the underlying mechanism for how organisms respond to temperature change.

Model derivation. Temperature changes the conformational entropy of proteins [22], which in turn determines the binding affinity of enzymes [23-24] and affects the flexibility/rigidity and stability of the activated enzyme-substrate complex and hence the reaction rate [24]. The resulting temperature dependence of the change in entropy, ΔS (with enthalpy and heat capacity remaining constant), is the simplest mechanism for giving rise to curvature in an Arrhenius plot and naturally leads via Eq. (3) to power law deviations from the simple exponential form [21]. Following [15], the change of entropy for a given change in temperature can be expressed as $Td\Delta S/dT = \Delta C$, where ΔC is the heat capacity of proteins. Integrating over temperature gives $\Delta S = \Delta S_0 + \Delta C \ln(T/T_0)$, where ΔS_0 is the entropy when $T = T_0$, an arbitrary reference temperature, commonly taken to be 298.15 K ($25°C$) (see Supplementary Text S3). Using this expression for ΔS in eq. (3), and after simplifying, we straightforwardly obtain (Supplementary Text S4):

$$k = \left(\frac{k_B}{h}\right)\left[e^{\frac{\Delta S_0}{R}} T_0^{\frac{-\Delta C}{R}}\right]\left(\frac{1}{T}\right)^{-(\frac{\Delta C}{R}+1)} e^{\frac{-\Delta H}{RT}} \tag{4}$$

Eq. (4) has the form of a classic Arrhenius-like exponential term, modified by a power-law, but with a different interpretation of the "effective activation energy" in terms of the change in enthalpy. The pattern described by Eq. (4) is a curved temperature response in an Arrhenius plot of $\ln k$ vs. T^{-1}:

$$\ln k = \ln\left(\frac{k_B}{h}\right)\left[e^{\frac{\Delta S_0}{R}} T_0^{\frac{-\Delta C}{R}}\right] - \left(\frac{\Delta H}{R}\right)T^{-1} - \left(\frac{\Delta C}{R}+1\right)\ln T^{-1} \tag{5}$$

Consequently, $d\ln k/dT^{-1} = -\Delta H/R - (\Delta C/R + 1)/T^{-1}$, leading to the extrema of $\ln k$ occurring at $T^{-1} = T_{ext}^{-1} = -(\Delta C + R)/\Delta H$ (see Supplementary Text S6). This is a minimum, i.e., the curve is concave upwards, or a "happy mouth", if $\Delta C > -R$, whereas it is a maximum, or a convex downwards "sad mouth", if $\Delta C < -R$. Furthermore, for T_{ext}^{-1} to be positive this requires $\Delta H < 0$ for a minimum or $\Delta H > 0$ for a maximum.

Several important points should be noted about our result:

First, its simple mathematical form, namely an exponential modified by a power law, coincides mathematically with an empirical phenomenological equation suggested by Kooij in 1893 [25]. However, our derivation provides an underlying mechanism for the origin of the expression and, consequently, for how its parameters are related to the thermodynamic variables. Our approach differs from previous expressions derived from considerations of chemical kinetics (Supplementary Text S1). For instance, a heuristic derivation inspired by a Maxwell-Boltzmann distribution predicts a similar expression but with a power law modification of $T^{1/2}$ rather than $T^{\frac{\Delta C}{R}+1}$ [12, 13]; apart from not having a mechanistic basis, this is unable to explain concave deviations.

Second. An important consequence of our derivation is that it shows that a change of entropy with temperature is both sufficient and necessary for simultaneously explaining both the convex and concave curvatures commonly observed in Arrhenius plots. Under a thermodynamic/informational interpretation, the decrease in enzyme rate with increasing entropy due to increasing temperature beyond the optimal, means that the disorder of the enzyme, and particularly of the active site, has reached a state that causes a decrease in the binding affinity to the ligands. In contrast, changes in enthalpy alone can only explain convex curvature but not concave. To see this explicitly, we express ΔH in terms of heat capacity in eq. (3), $\Delta H = \Delta H_0 - \Delta C(T - T_0)$, to obtain $k = \frac{k_B}{h} e^{\Delta S/R} \left(\frac{1}{T}\right)^{-1} e^{\left[\frac{\Delta H_0 - \Delta C(T-T_0)}{R}\right]\left(\frac{1}{T}\right)}$, which leads to $\ln k \propto \ln\left(\frac{1}{T}\right) - \left[\frac{\Delta H_0 + T_0 \Delta C}{R}\right]\left(\frac{1}{T}\right)$. Regardless of the sign of both ΔC and/or ΔH_0, this always results in a convex downwards curve and so cannot explain, nor accommodate, concavity. Hobbs et al. [26] included changes in both enthalpy and entropy with temperature and derived a significantly more complicated expression than ours based on TST. In contrast, the minimalist scenario developed here is one in which only changes in entropy with temperature need be considered.

Third. The above derivation was for reaction rates at the microscopic enzymatic scale. Following the argument in the MTE we now show how it can be extended to biological variables at multiple scales up through multicellular organisms to ecosystems. The most salient example is metabolic rate, B. In general, this is derived by appropriately summing and averaging over all enzymatic reaction rates contributing to metabolism - some connected in series, some in parallel - and then summing and averaging over all cells: symbolically, $B \propto \sum k \approx \overline{k}$. Assuming there is a dominant set of rate limiting reactions contributing to the production of ATP [18], then the temperature dependence of $\overline{k}$, and therefore B, can be approximated by an equation of the form of Eq. (4), but with the parameters being interpreted as averages, $\overline{\Delta H}$ and $\overline{\Delta C}$. This results in: $B \approx B_0 \left(\frac{T_0}{T}\right)^{\frac{-\overline{\Delta C}}{R}-1} e^{\frac{-\overline{\Delta H}}{R T_0}\left(\frac{T_0}{T}\right)}$, where B_0 is a normalization constant (see Supplementary Text 8).

Fourth. Care, however, has to be taken with the normalization constants, such as B_0 in the case of metabolic rate, since from Eq. (4), these would naively be proportional to the ratio of the two fundamental constants, k_B and h. The presence of Planck's constant, h, for microscopic enzymatic reactions appropriately reflects the essential role of quantum me-

chanics in molecular dynamics. On the other hand, for macroscopic processes, such as whole body metabolic rate, the averaging and summing over macroscopic spatio-temporal scales which are much larger than microscopic molecular scales must lead to a classical description decoupled from the underlying quantum mechanics and, therefore, must be independent of h. This is analogous to the way that the motion of macroscopic objects, such as animals or planets, are determined by Newton's laws and not by quantum mechanics, and therefore do not involve h. Formally, the macroscopic classical limit is, in fact, realised when $h \to 0$. The situation here is resolved by recognising that the partition function for the distribution of energies in the transition state of the reaction has not been explicitly included in Eq. (2). This is given by a Planck distribution which leads to an additional factor $(1-e^{-h\nu/k_BT})$ where ν is the vibrational frequency of the bond, as first pointed out by Herzfeld [27]. For purely enzymatic reactions discussed above this has no significant effect since $k_BT << h\nu$, resulting in Eq. (2). Multicellular organisms, however, correspond to the classical limit where $h \to 0$ so $k_BT >> h\nu$ and $(1 - e^{-h\nu/k_BT}) \to h\nu/k_BT$. Consequently, the resulting temperature dependence of macroscopic processes, such as metabolic rate, become independent of h, as they must, but lose a factor of T relative to the microscopic result, Eq. (4), so that

$$B \approx \tilde{B}_0 \left(\frac{1}{T}\right)^{\frac{-\overline{\Delta C}}{R}} e^{\frac{-\overline{\Delta H}}{RT}} \tag{6}$$

with the normalization constant, $\tilde{B}_0$, no longer depending on h. The corresponding extrema (either minima or maxima) in an Arrhenius plot now occur at $T^{-1} = T_{ext}^{-1} = -\overline{\Delta C}/\overline{\Delta H}$.

Fifth. The micro and macro results, Eqs. (4) and (6), can be combined into a single expression for the temperature dependence of any variable, $Y(T)$:

$$Y(T) \approx Y_0 \left(\frac{1}{T}\right)^{\frac{-\overline{\Delta C}}{R}-\alpha} e^{\frac{-\overline{\Delta H}}{RT}} \tag{7}$$

where $\alpha = 1$ for the molecular level and 0 otherwise (for reaction rates, Y_0 is given by Eq. (4)). The extrema occur at $T^{-1} = T_{ext}^{-1} = -(\overline{\Delta C} + \alpha R)/\overline{\Delta H}$. It should be noted that the thermodynamic parameters may have additional dependencies that make the forms of Eqs. (6) and (7) more complicated (see Supplementary Text S8).

In addition to quantitatively explaining the origin and systematic curvature of the Arrhenius plot, our model makes several further testable predictions that interrelate the key features of thermodynamic parameters (e.g. enthalpy and heat capacity), biological traits (e.g growth and metabolic rates), classic thermal traits (e.g. thermal range and optimum temperature), and environmental features (e.g. pH and salinity). These various predictions, exhibited in Extended Data Fig. 1, are summarized as follows:

i. The maximum (or minimum) value of any biological trait as a function of temperature.

ii. The scaling relationship between differences in rates (e.g., $Y(T_2)/Y(T_1)$) and differences in temperatures $(T_2 - T_1)$; see Extended Data Fig. 2.

iii. The scaling relationship between heat capacity and enthalpy resulting from the optimization of the rates (Extended Data Fig. 4).

iv. The linear relationship amongst all pairs of the key thermal traits of the temperature response curve such as the minimum, maximum, and optimum temperatures or thermal range (Extended Data Fig. 6).

v. The linear relationships between a given thermal trait and fundamental thermodynamic parameters such as enthalpy (Extended Data Fig. 7)

vi. The linear-log relationship between thermodynamic parameters and a variety of other environmental features such as pH and salinity (Extended Data Fig. 9).

vii. The relationship between thermal traits and environmental features such as between the optimal temperature and conductivity (Extended Data Fig. 9).

viii. All temperature response curves collapse onto a single universal curve after the appropriate rescaling given by our theoretical framework (see discussion below and Supplementary Text S7; Fig. 2; Extended Data Fig. 10).

Fitting the predictions of the model to temperature response curves data across levels of biological organization and taxa. To assess these predictions, we compiled a database of 57 studies encompassing 118 temperature-response curves including those which are explicitly predicted by biological theories such as the MTE. Our survey included data of different rates/times/properties in different environments ranging from psychrophilic to hyperthermophilic organisms and across all domains of life, including viruses, bacteria, archaea and unicellular and multicellular eukaryotes covering both ectotherms and endotherms (see Supplementary Methods). rescaled

We found that our model provides an excellent fit to a wide variety of temperature response data for rates and times, spanning individual to ecosystem-level traits across viruses, unicellular prokaryotes, and mammals (see Supplementary Table 2). Fig. 1 shows some representative examples of fits to convex patterns with long tails at low and high temperatures (Figs. 1a-f) as well as concave patterns (such as the temperature dependence of endotherm metabolism and biological times) also with tails at both ends. As discussed below, it should also be noted that the temperature response curve can be represented as a linear relationship using the rescaled form given in Equation S5.2 which compares well with data (Extended Data Fig. 2).

The values of the parameters ΔS_0, ΔH, and ΔC had skewed distributions (Extended Data Figure 3, Supplementary Table 2, 3). Prediction ii) also fits the data well showing that curved temperature responses can be simplified to a linear relationship for discrete measures of both rates and temperatures (Extended Data Fig. 2). Predictions iv-v) are well supported by a subset of the overall data (Extended Data Figs. 5, 6, and 7) and, below, we refer in more detail to predictions vi-viii.

Derivation of general equations for the variation in the parameters. In general, thermodynamic properties such as ΔS_0, ΔH, and ΔC are extensive variables which scale

with the size (e.g. mass) of a system. As such, they are expected to vary across taxa and levels of biological organization which we address in the Supplementary Material (see the Supplementary Text S10 and Tables S3-S5). In addition, these thermodynamic properties are expected to depend on factors other than temperature, as are the associated biological rates. We now show that our model can be extended to derive a general expression that predicts the dependency of biological rates and thermodynamic parameters on factors such as conductivity and pH. Keeping temperature constant in Eq. (4) (Supplementary Text S9) we express the biological rate as a function of an environmental variable, Z, such as pH or salinity: $k = f(Z)$. Thermodynamic parameters depend on Z in such a way that the generic form of the dependence of a thermal trait, τ, on Z is given by

$$\tau \propto b \ln Z \tag{8}$$

$$e^p = e^b Z^a \tag{9}$$

where p is a thermodynamic parameter, and a and b are parameters of the system. This relationship is motivated by examples for conductivity and salinity. For instance, from chemical kinetic theory k depends on salt concentration and in turn salt affects the electrical conductivity σ, a relationship that can be expressed as a power law: $k = m\sigma^n$ where the normalisation m and the exponent n are derived from molecular properties [28]. This leads via Eq. (5) to $e^p = e^b(\sigma)^a = e^b m^a \sigma^{na}$. To evaluate this prediction, we used six empirical curves for the temperature response of maximum plant germination rates at different conductivities (12.2-37.2 dS/m) [29] (Extended Data Fig. 8). For each of the thermodynamic parameters the fit of Eqs. (5) and (6) was significant ($P < 0.05$); Extended data figure 9, demonstrates that the variation commonly observed in the values of parameters that account for temperature responses can be explained by the action of a second explanatory variable, in this case conductivity (Supplementary Table S6). In general, the final form of Equations (8) and (9) would depend on the specific relationship between an environmental variable and k.

Universal scaling and data collapse. A powerful, but classic, method for exhibiting and testing the generality of a theory is to express it in terms of dimensionless variables which collapse the data onto a single "universal" curve across all scales. [e.g. 30]. To do so here, we introduce dimensionless rates, Y^*, and temperatures, T^*, by rescaling them by their values at the extremum, T_{ext}, where Y takes on either its minimum or maximum value, $Y_{ext} = Y(T_{ext})$:

$$Y^*(T^*) = \frac{Y(T)}{Y_{ext}}; \qquad T^* = \frac{T}{T_{ext}} \tag{10}$$

In terms of these rescaled variables, Eq. (4) reduces to the simple dimensionless form

$$Y^{*1/a} = T^* e^{1/T^* - 1}. \tag{11}$$

where $a = \overline{\Delta C}/R + \alpha$ with $\alpha = 0$ or 1, depending on whether the system is macro- or microscopic. Note that the extrema are given by $Y_{ext} = Y_0 T_{ext}^a e^{-b/T_{ext}}$ and $T_{ext} = -b/a$, where $b = \overline{\Delta H}/R$ (see Supplementary Material).

Our theory therefore predicts that when $Y^{*1/a}$ is plotted against $1/T^*$ all of the various rates regardless of the specific processes collapse onto a single parameterless curve whose simple functional form is given by Eq. (11). Notice that this optimises at $T^* = 1$ and encompasses in the same curve both the convex and concave behaviours predicted in the original Arrhenius plot as a function of T. In that regard, note also that the function $\hat{Y}^*(T^*) \equiv (e/T^*)^a Y^*(T^*) = e^{a/T^*}$ is predicted to be of a "pure" Arrhenius form as a function of T^*. Thus, a plot of $\ln \hat{Y}^*(T^*)$ vs. $1/T^*$ should yield a straight line with slope a (see Supplementary Material).

Our prediction of the universal curve is very well supported by data, as illustrated in Figs. 2a, b where the collapse of all the data from this study for both convex and concave patterns regardless of organizational level, temperature range or taxa are shown. This result strongly supports the idea that our model captures all of the meaningful dimensions of thermodynamic and temperature variation for diverse biological properties, which can ultimately be viewed as a single exponential relationship.

Conclusion. In conclusion, we have derived a mechanistic yet simple model for biological temperature responses. Our model is a general extension of the EEP equation, but unlike previous models requires only entropy to vary with temperature, presumably due to an optimization. We do not imply that temperature is the only variable determining biological rates. We acknowledge the importance of including other variables that could be more limiting than temperature in certain environments, such as pH and salinity, which also determine enzymatic and other rates at higher levels of organization [31]. However, we have shown how these features can be incorporated into our framework. Importantly, our model applies to any biological rate at any biological scale. It provides a good fit to data across organization level, environment and taxa, including groups such as endotherms, thermophiles, and hyperthermophiles. This framework is scalable. For example, further extensions could include time, other variables to predict the thermodynamic parameters or vice versa (i.e. the parameters could explain biological traits), and future connections could and should be made with non-equilibrium thermodynamics [32].

References

1. Noll P, Lilge L, Hausmann R, Henkel M (2020) Modeling and exploiting microbial temperature response. Processes 8: 121.

2. Rezende EL, Bozinovic F, Szilágyi A, Santos M (2020) Predicting temperature mortality and selection in natural Drosophila populations. Science 369(6508):1242-1245.

3. Schulte PM, Healy TM, Fangue NA (2011) Thermal performance curves, phenotypic plasticity, and the time scales of temperature exposure. Integr Comp Biol 51(5):691-702.

4. Yap TF, Liu Z, Shveda RA, Preston DJ (2020) A predictive model of the temperature-dependent inactivation of coronaviruses. Appl Phys Let 117(6): 060601.

5. Dell AI, Pawar S, Savage VM (2011) Systematic variation in the temperature dependence of physiological and ecological traits. Proc Natl Acad Sci U S A. 108(26):10591-6.

6. Ghjuvan Grimaud, Francis Mairet, Antoine Sciandra, Olivier Bernard (2017) Modeling the temperature effect on the specific growth rate of phytoplankton: a review. Rev Environ Sci Biotechnol 16: 625–645.

7. Brown JH, Gillooly JF, Allen AP, Savage VM, West GB (2004) Toward a metabolic theory of ecology. Ecology 85(7):1771-1789.

8. Arrhenius SA (1889) Über die reaktionsgeschwindigkeit bei der inversion von rohrzucker durch säuren. Z Phys Chem 4: 226–248.

9. Laidler KJ (1984) The development of the Arrhenius equation. J Chem Educ 61(6):494.

10. Laidler KJ, and King MC (1983) The development of transition-state theory. J Phys Chem 87(15)2657–2664.

11. Price CA, Weitz JS, Savage VM, Stegen J, Clarke A, Coomes DA, et al. (2012) Testing the metabolic theory of ecology. Ecol Lett 15(12):1465-74.

12. Eyring H (1935) The activated complex in chemical reactions. J Chem Phys 3: 107.

13. Evans MG, Polanyi M (1935) Some applications of the transition state method to the calculation of reaction velocities, especially in solution. Trans Faraday Soc 31: 875.

14. Zhou HX (2010) Rate theories for biologists. Q Rev Biophys 43(2):219–293.

15. Prabhu NV and Sharp KA (2005) Heat capacity in proteins. Annu Rev Phys Chem 56:521-48.

16. Daniel RM, Danson MJ, Eisenthal R (2001) The temperature optima of enzymes: a new perspective on an old phenomenon. Trends Biochem Sci 26: 223–225.

17. DeLong JP, Gibert JP, Luhring TM, Bachman G, Reed B, Neyer A et al (2017) The combined effects of reactant kinetics and enzyme stability explain the temperature dependence of metabolic rates. Ecol Evol 7(11):3940–3950.

18. Gillooly JF, Brown JH, West GB, Savage VM, Charnov EL (2001) Effects of size and temperature on metabolic rate. Science 293(5538):2248-51.

19. Porter WP, Kearney M (2009) Size, shape, and the thermal niche of endotherms. Proc Natl Acad Sci U S A 106 Suppl 2:19666-72.

20. Klales A, Duncan J, Nett EJ, Kane SA (2012) Biophysical model of prokaryotic diversity in geothermal hot springs. Phys Rev E Stat Nonlin Soft Matter Phys 85(2 Pt 1):021911.

21. Sturtevant JM (1977) Heat capacity and entropy changes in processes involving proteins. Proc Natl Acad Sci U S A 74(6):2236–2240.

22. Wallin S and Chan HS (2009) Conformational entropic barriers in topology-dependent protein folding: perspectives from a simple native-centric polymer model. J Phys Condens Matter 21 329801.

23. Frederick KK, Marlow MS, Valentine KG, Wand AJ (2007) Conformational entropy in molecular recognition by proteins. Nature 448: 325–329.

24. Tzeng S-R and Kalodimos CG (2012) Protein activity regulation by conformational entropy. Nature 488(7410):236-40.

25. Kooij DM (1893) Uber die zersetzung des gasförmigen phosphorwasserstoffs. Z Phys ChemAbt B 12:155.

26. Hobbs JK, Jiao W, Easter AD, Parker EJ, Schipper LA and Arcus VL (2013) Change in heat capacity for enzyme catalysis determines temperature dependence of enzyme catalyzed rates. ACS Chem Biol 8: 23882393.

27. Herzfeld KF (1919) Zur Theorie der Reaktionsgeschwindigkeiten in Gasen. Ann Phys 59:635–667.

28. Park C and Raines RT (2001) Quantitative analysis of the effect of salt concentration on enzymatic catalysis. J Am Chem Soc 123: 11472-11479.

29. Esechie HA (1993) Interaction of salinity and temperature on the germination of alfalfa cv CUF 101. Agronomie 13: 301-306

30. West, GB, Brown JH, Enquist BJ (2001) A general model for ontogenetic growth. Nature 413(6856): 628.

31. Rektorschek M, Weeks D, Sachs G, Melchers K (1998) Influence of pH on metabolism and urease activity of Helicobacter pylori. Gastroenterology 115(3):628-41.

32. Demirel Y, Gerbaud V (2018) Nonequilibrium thermodynamics: transport and rate processes in physical and biological systems. 4th Edition. Elsevier

Methods

Details on mathematical derivation, database compilation and estimation of parameters for the models are in Supplementary Methods.

Data and code availability

The database and (R) code will be available in a public repository after acceptance. During the review process, data and code can be provided upon request.

Acknowledgements

We thank authors that contributed with raw data. JIA was supported by a Beca de Doctorado Nacional CONICYT 21130515. PAM was supported by projects AFB 17008 and FONDECYT 1161023. JIA and GBW were supported by NSF 1838420, JIA and CPK were supported by NSF 1840301, GBW and CPK were supported by the Charities Aid Foundation of Canada (CAF) for the grant entitled 'Toward Universal Theories of Ecological Scaling'. BD acknowledges support from projects ANID-FONDECYT 1150171 and 1190998.

Author contributions.

JIA and PM conceived the paper. JIA, CK, GW, and PM, derived the model. JIA compiled the database and made the statistical analysis. JIA, BD, CK, GW, PM wrote the paper.

Competing interests.

The authors declare no competing interests.

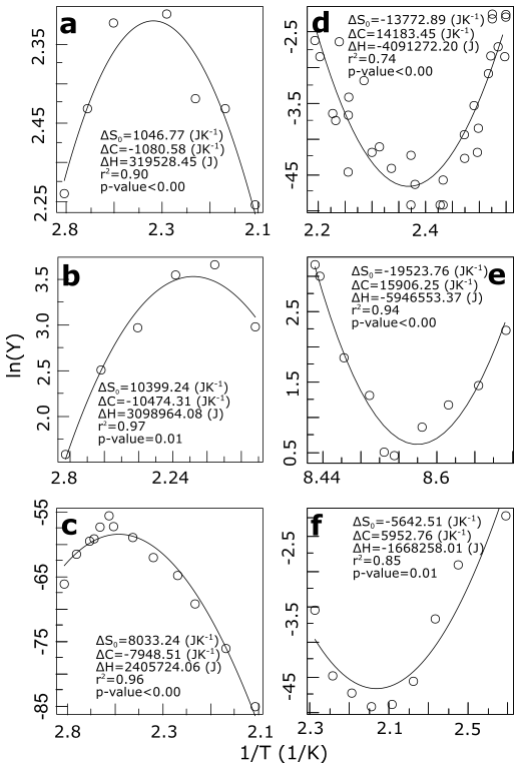

Figure 1. Temperature response curves fitted to Eq.5 for a wide diversity of biological examples. (a)-(c) convex patterns and (d)-(f) concave patterns. (a) metabolic rate in the multicellular insect *Blatella germanica*, (b) maximum relative germination in alfalfa (for a conductivity of 32.1 dS/m), (c) growth rate in *S. cerevisiae*, (d) mortality rate in the fruit fly (*Drosophila sukii*), (e) generation time in strain 121, (f) metabolic rate in the rodent *Spermophilus parryii*. The abscissa is in units of $(1/T) * 10^{-3}$. For references see Supplementary Methods.

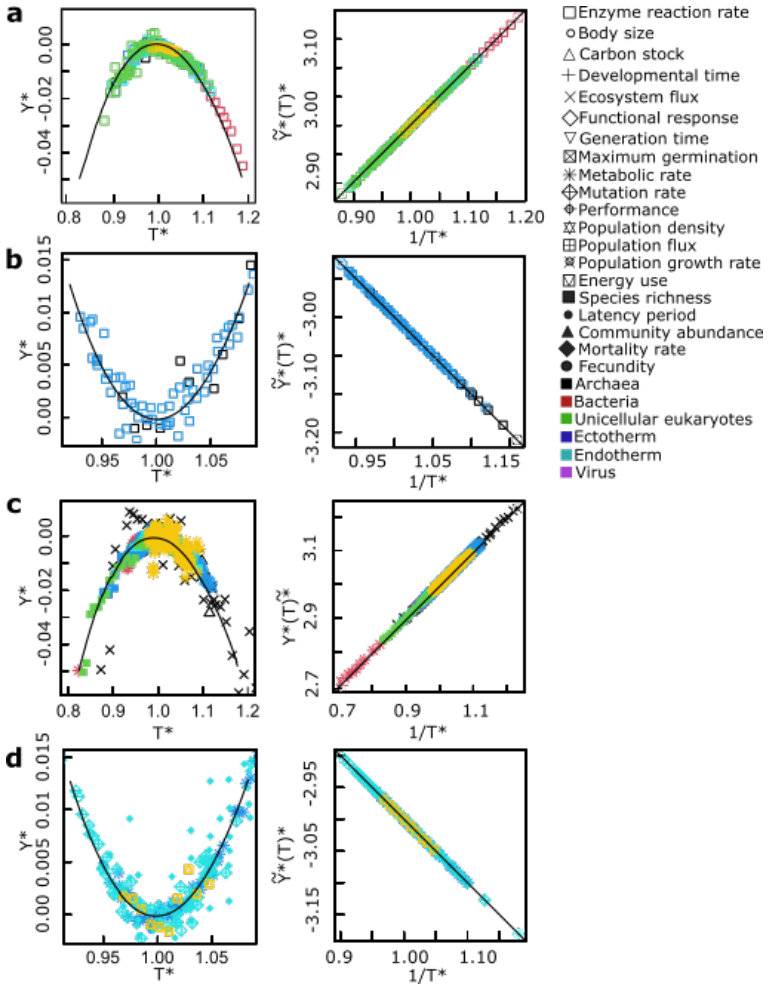

Figure 2. Universal patterns of temperature response in non-linear (right panels) and linear (left panels) forms. (a) concave patterns at the molecular (enzymatic) level, and (b) convex patterns at the molecular level, (c) concave patterns above the molecular level, and (d) convex patterns above the molecular level. Rescaling based on Eq. 11 showing the universal temperature-dependence of data from Fig.1 combined with additional compiled studies. All curves regardless of variable, environment and taxa collapse onto a single curve. Inner panels depict an alternative linear data collapse based on Eq. S7.14.